GALVANOSTATIC CYCLING OF VANADIUM OXIDE (V_6O_{13}) IN A NONAQUEOUS SECONDARY LITHIUM CELL

E. J. FRAZER and S. PHANG*

CSIRO Institute of Energy and Earth Resources, Division of Mineral Chemistry, P.O. Box 124, Port Melbourne, Victoria 3207 (Australia)

(Received March 5, 1982)

Summary

The galvanostatic cycling of Li(Al)–V_6O_{13} cells in 1M $LiAsF_6$/propylene carbonate (PC)–acetonitrile (AN) and 1M $LiAsF_6$/PC electrolytes is reported. The discharge capacity and voltage of the Li(Al)–V_6O_{13} cell were shown to be consistently higher than those of the corresponding Li(Al)–TiS_2 cell. Discharge rates of 1.2, 2.5, 5.0 and 10.0 mA cm^{-2} with active material utilisations of 20 - 60% were obtained from the Li(Al)–V_6O_{13} cell. The addition of fresh PC–AN electrolyte resulted in an improvement in cell capacity, but did not stop capacity decline on cycling. Cycle life of Li(Al)–V_6O_{13} cells was normally less than 50 cycles. It was also found that exposure of the V_6O_{13} electrode to moist air reduced the OCV and the discharge capacity of the cell. Short circuiting and complete discharge of the cell resulted in lower capacity and this may have been due to some degree of irreversible reduction of the V_6O_{13}.

Introduction

Transition metal oxides are being evaluated for lithium cells in numerous laboratories because of their characteristics of safety, economy, high energy density, and long life. Some of the oxides being investigated include V_2O_5 [1, 2], MoO_3 [2 - 5], MnO_2 [5, 6], TiO_2 [2, 7], Cr_2O_3 [8] and V_6O_{13} [9]. Our attention was drawn to V_6O_{13} because of its large theoretical energy density (~ 800 W h kg^{-1}), its excellent rechargeability, and its ease of preparation [9].

The crystal structure of V_6O_{13} was first determined by Aebi [10] and later refined by Wilhelmi *et al.* [11]. The structure can be visualised as composed of distorted octahedra, connected by shared corners and edges with V–O distances in the range 1.642 - 2.276 Å. Vanadium oxide (V_6O_{13}) is metallic and can reversibly incorporate lithium topochemically at room temperature [12]. Although eight lithium ions can be reversibly intercalated

*Now at Karratha College, P.O. Box 315, Karratha, Western Australia 6714, Australia.

0378-7753/83/$3.00

per V_6O_{13} formula unit, highly lithiated V_6O_{13} is a poor electronic conductor [13]. Therefore, use of conducting diluents such as graphite is usually necessary.

Two methods for the preparation of V_6O_{13} to be used as a cathode material have been described by Murphy *et al.* [9]. In the first method stoichiometric proportions of V_2O_5 and V metal were reacted at 650 °C. In the second method, NH_4VO_3 was thermally decomposed below 450 °C in an inert atmosphere. The first method produced V_6O_{13} of particle size 10 to 50 μm, while the second method produced particle sizes of 1 - 5 μm with stoichiometries ranging from $VO_{2.17}$ to $VO_{2.20}$. However, the materials from both methods gave similar XRD patterns. Murphy *et al.* [9] reported that V_6O_{13} prepared using the thermal decomposition method gave electrochemical cells of higher capacity, probably because of the smaller particle size.

In this paper we investigate the performance of Li(Al)–V_6O_{13} cells principally using 1M $LiAsF_6$/PC–AN. This electrolyte was previously evaluated for the lithium electrode [14] and various primary and secondary lithium cells [15, 16]. The performance of the V_6O_{13} cell is also compared with the corresponding TiS_2 cell in both 1M $LiAsF_6$/PC and 1M $LiAsF_6$/PC–AN.

Experimental

Vanadium oxide (V_6O_{13}) was prepared using the method described by Murphy *et al.* [9]. Ammonium metavanadate (Cerac Inc., USA, 99.99% pure) was thermally decomposed by heating in a flowing argon atmosphere at 150 °C for ~ 12 h and at 400 °C for two days. An XRD analysis of the product revealed some traces of V_2O_5 (< 5%) in the V_6O_{13}. The range of particle size of the V_6O_{13} as determined by SEM was 1 - 20 μm.

The purification of PC, AN and $LiAsF_6$ has been described elsewhere [14 - 16]. In this work another procedure for purifying AN [17] was also employed. Acetonitrile was first dried with a mixture of 4A and 5A molecular sieves for ~ 2 weeks, followed by ~ 1 week with CaH_2, and then distilled over CaH_2.

The V_6O_{13} electrodes were made by hot-pressing (at ~ 150 °C, 5000 psi) a mixture of V_6O_{13} (70% w/w), powdered graphite (20% w/w) and polyethylene (10% w/w) onto a 2 cm square nickel grid. The anode was constructed by pressing lithium–aluminium (90–10 at.%) foil (Foote Mineral Company, USA) on to a nickel grid of similar dimensions. The V_6O_{13} electrode was sandwiched between two lithium–aluminium electrodes and separated from each using a microporous polypropylene film (Celgard 2400, Celanese Corporation, USA). The electrodes were then held firmly in parallel plate configuration inside a Teflon cell filled with electrolyte. The cells were cycled between the preset voltages of 1.5 and 2.6 V (in some cases, 1.5 and 2.9 V) at room temperature (~ 23 °C) using the apparatus described previously [16]. Since lithium was present in excess, the term "active material utilisation" refers to the utilisation of the V_6O_{13}.

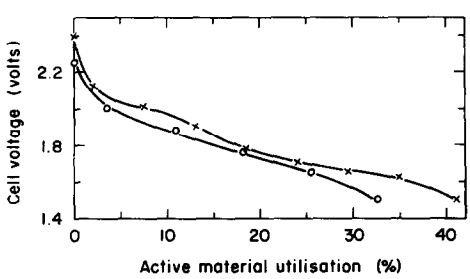

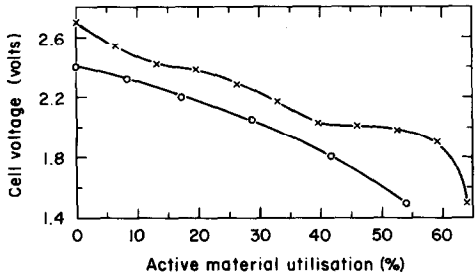

Fig. 1. Discharge characteristics of the Li(Al)–V_6O_{13} cell compared with that of the Li(Al)–TiS_2 cell in 1M $LiAsF_6$/PC (i_d = 0.12 mA cm^{-2}). ○, TiS_2 = 57.3 mg; ×, V_6O_{13} = 219 mg.

Fig. 2. Discharge characteristics of the Li(Al)–V_6O_{13} cell compared with that of the Li(Al)–TiS_2 cell in 1M $LiAsF_6$/PC–AN (i_d = 1.2 mA cm^{-2}). ○, TiS_2 = 48.3 mg; ×, V_6O_{13} = 182 mg.

Results and discussion

(i) Comparison of Li(Al)–V_6O_{13} and Li(Al)–TiS_2 cells

Murphy *et al.* [9] studied the Li/1M $LiAsF_6$, PC/V_6O_{13} cell at low currents (0.2 mA). The active material utilisation was estimated to be ~ 50% and ~ 70% for the V_6O_{13} produced by the elemental and decomposition method, respectively. In this work we obtained ~ 40% active material utilisation for the Li(Al)/1M $LiAsF_6$, PC/V_6O_{13} cell and ~ 64% for the Li(Al)/1M $LiAsF_6$, PC–AN/V_6O_{13} cell at discharge rates of 0.12 and 1.2 mA cm^{-2}, respectively (see Figs. 1 and 2). However, a proper comparison with the work of Murphy *et al.* [9] could not be made because the current density used was not quoted.

It was observed that the OCV decreased by ~ 200 mV to a steady value over a period of hours after cell assembly. The OCV of the Li(Al)–V_6O_{13} cell containing 1M $LiAsF_6$/PC–AN and 1M $LiAsF_6$/PC electrolytes was 2.9 and 3.2 V, respectively. The OCV of Li(Al)–TiS_2 cells containing the same electrolytes was found to be 2.8 and 3.2 V, respectively. The higher OCV in the 1M $LiAsF_6$/PC electrolyte was of little advantage because reasonable active material utilisation (~ 35%) could only be achieved at low discharge rates (compare Figs. 1 and 2). In this work the theoretical energy densities of V_6O_{13} and TiS_2 are based on the limiting stoichiometries of $Li_8V_6O_{13}$ and $LiTiS_2$, respectively [13, 18]. The theoretical specific capacities are therefore 417 and 239 A h kg^{-1}, respectively. In Fig. 2 it can be seen that in PC–AN the active material utilisation and voltage of the Li(Al)–V_6O_{13} cell are generally higher than that of the corresponding Li(Al)–TiS_2 cell. In the case of the Li(Al)–V_6O_{13} cell poor voltage regulation was indicated. In fact, two plateaus were observed, one at ~ 2.4 V and another at ~ 2.0 V, suggesting complexities in the Li(Al)–V_6O_{13} phase diagram. The specific capacities of V_6O_{13} and TiS_2 calculated from the data of Fig. 2 are 270 and 130 A h kg^{-1}, respectively.

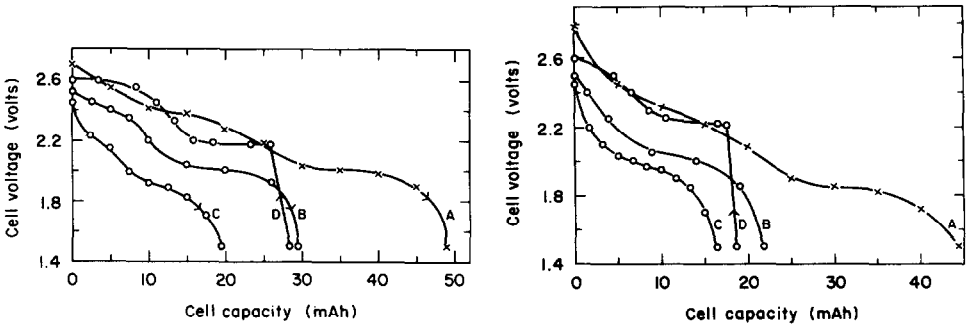

Fig. 3. Discharge characteristics of the Li(Al)–V_6O_{13} cell in 1M $LiAsF_6$/PC–AN (i_d = 1.2 mA cm^{-2}, i_c = 0.06 mA cm^{-2} and V_6O_{13} = 182 mg). A, first discharge; B, second discharge; C, fifth discharge; D, first charge.

Fig. 4. Discharge characteristics of the Li(Al)–V_6O_{13} cell in 1M $LiAsF_6$/PC–AN (i_d = 1.2 mA cm^{-2}, i_c = 0.25 mA cm^{-2} and V_6O_{13} = 179 mg). A, first discharge; B, second discharge; C, fourth discharge; D, first charge.

(ii) Discharge characteristics and rechargeability

The discharge characteristics of two Li(Al)–V_6O_{13} cells containing 1M $LiAsF_6$/PC–AN are shown in Figs. 3 and 4. Each cell contained ~ 180 mg of V_6O_{13} and each was discharged at 1.2 mA cm^{-2}. However, one cell (Fig. 3) was charged at 0.06 mA cm^{-2}, while the other (Fig. 4) was charged at 0.25 mA cm^{-2}; the preset voltage cut-off was 2.6 V in both cases.

From the initial discharge curves (curves A) the active material utilisations were found to be 64% (Fig. 3) and 58% (Fig. 4). The charge curves (curves D) were of similar shape, but the amount of charge returned to the cell was dependent on the charging rate. The charging capacities of 28.4 mA h (Fig. 3) and 18.6 mA h (Fig. 4) corresponded to rechargeabilities of 58% and 42%, respectively. Subsequent discharge of the cells (curves B) yielded active material utilisations of ~ 39% (Fig. 3) and ~ 29% (Fig. 4), corresponding to ~ 60% and ~ 50% of the respective initial discharge capacities. Both capacities decreased to 35 - 40% of the initial by the 4th and 5th discharge (curves C) showing no major dependence on charging rate.

(iii) The effect of discharge rate on active material utilisation

Figure 5 shows four initial discharge curves obtained from Li(Al)/1M $LiAsF_6$, PC–AN/V_6O_{13} cells at 1.2, 2.5, 5.0, and 10.0 mA cm^{-2}. As expected, the active material utilisation decreased with an increase in the discharge rate. The two voltage plateaus normally present (curves A - C) were not observed at 10 mA cm^{-2} (curve D). In the latter case, the instantaneous voltage drop at the beginning of discharge was ~ 0.5 V. Figure 6 shows the current density plotted against the active material utilisation (data from Fig. 5). A linear relationship has also been suggested for Li–TiS_2 cells by Gaines *et al.* [19], although there is no theoretical basis for this behaviour.

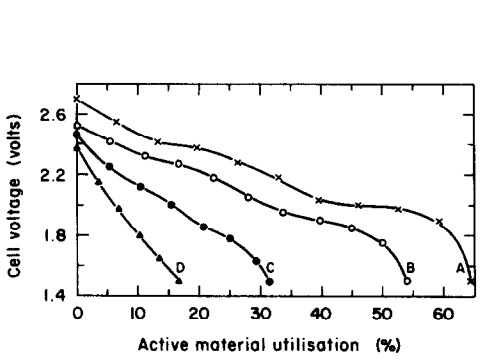

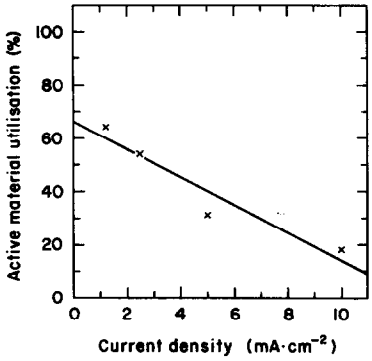

Fig. 5. Initial discharge characteristics of the Li(Al)–V_6O_{13} cell in 1M $LiAsF_6$/PC–AN at different discharge rates. A, i_d = 1.2 mA cm^{-2}, V_6O_{13} = 182 mg; B, i_d = 2.5 mA cm^{-2}, V_6O_{13} = 142 mg; C, i_d = 5.0 mA cm^{-2}, V_6O_{13} = 158 mg; D, i_d = 10.0 mA cm^{-2}, V_6O_{13} = 191 mg.

Fig. 6. Plot of current density *vs.* active material utilisation for the Li(Al)–V_6O_{13} cell in 1M $LiAsF_6$/PC–AN.

(iv) The effect of moist air on the V_6O_{13} electrode

Many oxides used in batteries exhibit moisture sensitivity and this can cause serious technological problems such as loss of strength and conductivity of the material [20]. In order to test the sensitivity of V_6O_{13} to moisture, one of the V_6O_{13} electrodes was exposed for ~ 24 h to an atmosphere of relative humidity ~ 59%. Figure 7 compares the discharge characteristics of lithium cells made with exposed and unexposed electrodes. Both cells contained ~ 140 mg of V_6O_{13} and were cycled at the same rates in the 1M $LiAsF_6$/PC–AN electrolyte. The cell using the exposed electrode had an OCV of 2.6 V compared with 2.9 V for that using the unexposed electrode. The cell using the exposed electrode gave an active material utilisation of ~ 34% for the initial discharge, ~19% for the 2nd discharge, and ~5% for the 8th discharge. By comparison, the cell using the unexposed electrode gave an

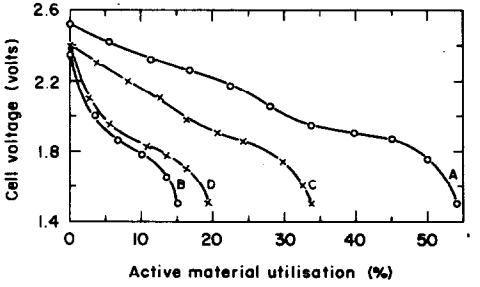

Fig. 7. Discharge characteristics of the Li(Al)–V_6O_{13} cell in 1M $LiAsF_6$/PC–AN (i_d = 2.5 mA cm^{-2}, i_c = 0.63 mA cm^{-2}). A, first discharge; B, tenth discharge of an unexposed electrode (V_6O_{13} = 142 mg). C, first discharge; D, second discharge of an exposed electrode (V_6O_{13} = 148 mg).

active material utilisation of ~54% for the initial discharge and ~15% for the 10th discharge. Evidently, it is deleterious to cell performance to expose V_6O_{13} electrodes to a moist atmosphere, and therefore controlled atmosphere fabrication procedures would be necessary in practice.

(v) The influence of the PC–AN electrolyte on cell performance

On prolonged cycling the PC–AN electrolyte changed colour from colourless to light orange. This phenomenon suggested some deterioration of the electrolyte. Figure 8 shows that the addition of fresh electrolyte substantially improved the capacity of the Li(Al)/1M $LiAsF_6$, PC–AN/V_6O_{13} cell.

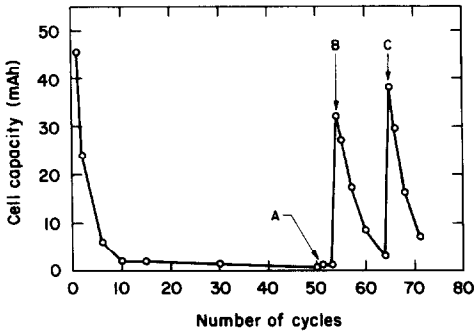

Fig. 8. The effects of electrolyte on cell capacity (i_d = 1.2 mA cm^{-2}, i_c = 0.25 mA cm^{-2}, V_6O_{13} = 231 mg, cell cycled between 1.5 and 2.9 V). A, cell rested for ~ 4 h; B, cell rested for ~ 18 h in fresh electrolyte; C, cell rested for ~ 4 h in fresh electrolyte.

The data of Fig. 8 were obtained by cycling the cell between the preset voltages of 2.9 and 1.5 V. The higher preset charging voltage used here did not noticeably improve discharge capacity. Under these conditions, the capacity decreased rapidly so that by the 50th cycle the cell was almost spent, with a capacity of ~ 0.5 mA h. Even allowing an ~ 4 h rest period before charging, cycles 51 and 53 (point A) showed only marginal improvement. The cell was then rinsed and refilled with fresh electrolyte and rested for ~ 18 h. The rinsing procedure was facilitated by cutting off a small piece of the lower corner of the polypropylene separator bag to allow draining. The cell was again charged at 0.25 mA cm^{-2} to 2.9 V and then discharged. As indicated by B, an improvement in cell capacity was obtained. However, the capacity of the cell then decreased with cycling in much the same manner as experienced earlier. Again, resting the cell (for ~ 3 days) did not improve the discharge capacity. The cell was then rinsed and the electrolyte replaced a second time. The cell was finally rested for ~ 4 h and then charged in the normal way. An increase in discharge capacity was again obtained (point C), followed by yet another decline in capacity.

Figure 9 shows some SEM photographs of the electrode surfaces before and after cycling. Figure 9(a) shows the surface of a piece of the Li(Al) foil after it was pressed onto a nickel gauze grid. After cycling until cell failure, the surface was covered by a wax-like layer or film which is shown in Fig.

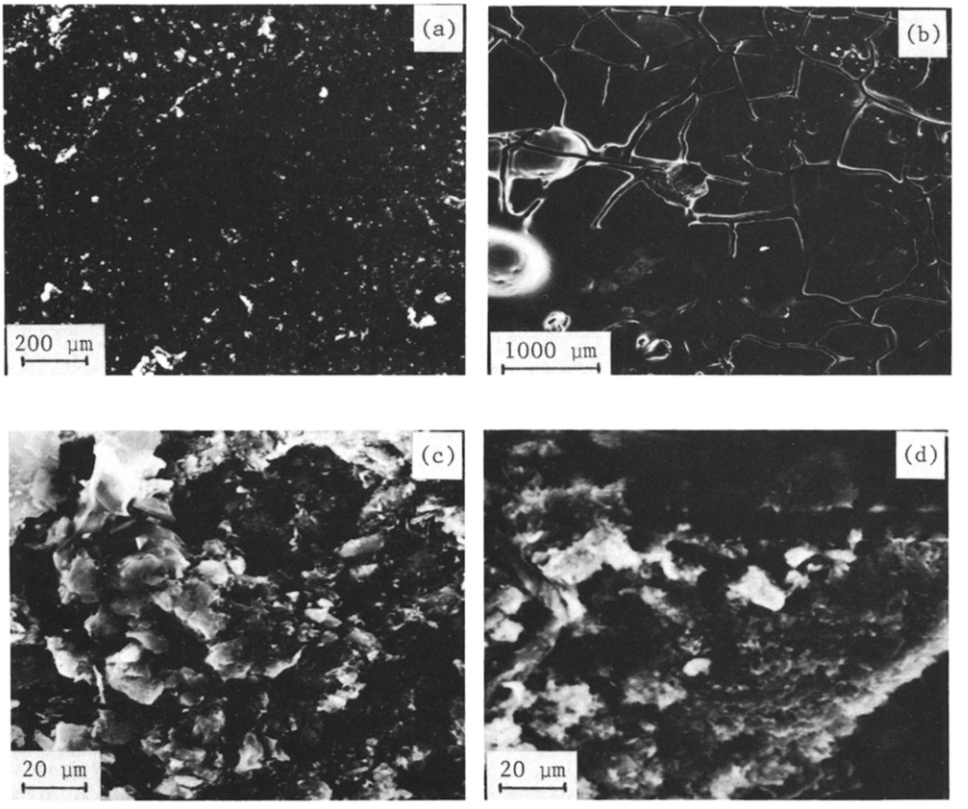

Fig. 9. (a) SEM photograph of an Li(Al) surface before cycling. (b) SEM photograph of an Li(Al) surface after cycling until cell failure (~ 50 cycles). (c) SEM photograph of a V_6O_{13} electrode surface before cycling. (d) SEM photograph of a V_6O_{13} electrode surface after cycling until cell failure (~ 30 cycles).

9(b). The cracked appearance of the surface may be due to the evaporation of the electrolyte. Polymeric layers on lithium and lithium–aluminium electrodes after cycling in PC electrolytes have also been detected by Epelboin *et al.* [21]. Dey [22] has reviewed the protective nature of film formation on lithium surfaces in some nonaqueous primary lithium batteries. However, the films which appeared here were detrimental to the secondary cell performance. Based on the observations discussed above (Fig. 8) it appears that fresh electrolyte may modify or partially remove the surface film resulting in improved cell capacities in the short term.

Figure 9(c) and 9(d) are SEM photographs of the V_6O_{13} electrode before and after cycling, respectively. The photographs show that the graphite, polyethylene binder, and V_6O_{13} were uniformly mixed to give an electrode with a large surface area. No major morphological changes were apparent after prolonged cycling.

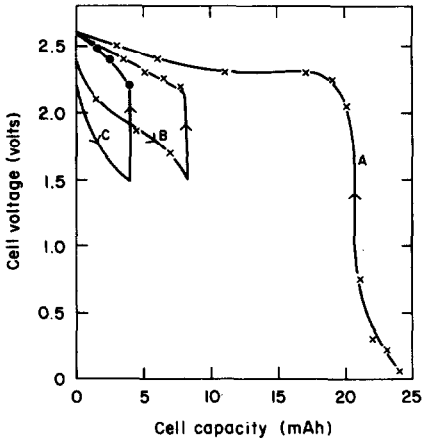

Fig. 10. Charge–discharge characteristics of the Li(Al)–V_6O_{13} cell in 1M $LiAsF_6$/PC–AN showing the effects of short-circuiting (i_d = 1.2 mA cm^{-2}, i_c = 0.25 mA cm^{-2}, V_6O_{13} = 195 mg). A, first charge; B, second discharge; C, 30th discharge.

(vi) Short-circuiting of cells

Murphy and Christian [13] have claimed that the Li/$LiAsF_6$, PC/V_6O_{13} cell may be temporarily short-circuited without irreversible reduction of the V_6O_{13}. It was therefore considered appropriate to test the Li(Al)/1M $LiAsF_6$, PC–AN/V_6O_{13} cell with respect to short-circuiting and the results of such a test are shown in Fig. 10. A short-circuited cell was left overnight; the completely discharged cell had an OCV of 0.07 V. It was then charged at 0.25 mA cm^{-2} (curve A) and discharged at 1.2 mA cm^{-2} giving a capacity of 8.5 mA h (~ 10% active material utilisation). This value is much lower than that usually obtained on the second cycle (~ 29%, curve B in Fig. 4) and this decrease may have been due to a degree of irreversible reduction of the V_6O_{13} on short-circuiting. While the capacity was reduced prematurely, the cell could still be cycled normally. However, by the 30th cycle (curve C) the discharge capacity had decreased to 4 mA h (~ 5% active material utilisation).

Conclusions

It has been shown that the specific capacity of V_6O_{13} is much larger (~ twice) than that of TiS_2 in the 1M $LiAsF_6$/PC–AN electrolyte. Furthermore, the higher density of V_6O_{13} (3.91 g cm^{-3}) can produce higher values of volumetric capacity and energy. Unlike the Li(Al)–TiS_2 cell, the discharge curve of the Li(Al)–V_6O_{13} cell displayed two voltage plateaus indicating multiphase complexities. The Li(Al)–V_6O_{13} cell showed superior performance compared with the Li(Al)–TiS_2 cell in the 1M $LiAsF_6$/PC–AN electrolyte where higher discharge rates were possible with good active material utilisation. Cycle life was, however, disappointing (< 50 cycles) and seems to be related to the formation of a film on the lithium electrode.

Fresh electrolyte apparently modified or partially removed the film and larger discharge capacities were obtained for several cycles. Exposure of the V_6O_{13} electrode to moist air reduced the OCV of the Li(Al)–V_6O_{13} cell from ~ 2.9 V to ~ 2.6 V and substantially decreased the discharge capacity. Short-circuiting and complete discharge of the cell also adversely affected cell performance, although the cell could still be cycled at low capacity.

Acknowledgements

Support was provided under the National Energy Research, Development and Demonstration Program administered by the Australian Department of National Development. The authors also thank K. Harris for SEM assistance, R. J. Hill for XRD analyses, and W. Kennedy for technical assistance.

References

1 C. R. Walk and J. S. Gore, *Ext. Abstr., Vol. 75-1,* Electrochemical Society, Princeton, NJ, 1975, p. 60.
2 M. S. Whittingham and M. B. Dines, *J. Electrochem. Soc., 124* (1977) 1388.
3 L. Campanella and G. Pistoia, *J. Electrochem. Soc., 118* (1971) 1905.
4 J. O. Besenhard and R. Schöllhorn, *J. Power Sources, 1* (1976) 267.
5 F. W. Dampier, *J. Electrochem. Soc., 121* (1974) 656.
6 H. Ikeda, T. Saito and H. Tamura, *Proc. Manganese Dioxide Symposium, Cleveland, 1975,* Vol. 1, Electrochemical Soc. Inc., Cleveland, OH, p. 384.
7 T. Ohzuku, Z. Takehara and S. Yoshizawa, *Electrochim. Acta, 24* (1979) 219.
8 J. O. Besenhard and R. Schöllhorn, *J. Electrochem. Soc., 124* (1977) 968.
9 D. W. Murphy, P. A. Christian, F. J. DiSalvo and J. N. Carides, *J. Electrochem. Soc., 126* (1979) 497.
10 F. Aebi, *Helv. Chim. Acta, 31* (1948) 8.
11 K. -A. Wilhelmi, K. Walterson and L. Kihlborg, *Acta Chem. Scand., 25* (1971) 2675.
12 G. L. Holleck, K. M. Abraham and S. B. Brummer, in B. B. Owens and N. Margalit (eds.), *Proc. Symp. Power Sources for Biomedical Implantable Applications and Ambient Temperature Lithium Batteries,* Vol. 80-4, Electrochemical Society, Princeton, NJ, 1980, p. 384.
13 D. W. Murphy and P. A. Christian, *Science, 205* (1979) 651.
14 A. J. Parker, P. Singh and E. J. Frazer, *J. Power Sources, 10* (1983) 1.
15 K. Cedzynska, A. J. Parker and P. Singh, *J. Power Sources, 10* (1983) 13.
16 E. J. Frazer and S. Phang, *J. Power Sources, 10* (1983) 23.
17 G. Forcier and J. Olver, *Anal. Chem., 37* (1965) 1447.
18 M. B. Dines, *Mater. Res. Bull., 10* (1975) 287.
19 L. H. Gaines, R. W. Francis, G. H. Newman and B. M. L. Rao, *Proc. 11th Intersoc. Energy Conv. Eng. Conf.,* Lake Tahoe, Nevada, 1976, AIChE, New York, p. 418.
20 L. M. Foster and G. V. Arbach, *J. Electrochem. Soc., 124* (1977) 164.
21 I. Epelboin, M. Froment, M. Garreau, J. Thevenin and D. Warin, *J. Electrochem. Soc., 127* (1980) 2100.
22 A. N. Dey, *Thin Solid Films, 43* (1977) 131.